JOURNAL OF AIRCRAFT
Vol. 44, No. 5, September–October 2007

Active Tiltrotor Whirl–Flutter Stability Augmentation Using Wing-Flaperon and Swash-Plate Actuation

Jinho Paik,* Rupinder Singh,* and Farhan Gandhi†
Pennsylvania State University, University Park, Pennsylvania 16802
and
Eric Hathaway‡
The Boeing Company, Philadelphia, Pennsylvania 19142

DOI: 10.2514/1.20234

This paper examines the effectiveness of active control through wing-flaperon and swash-plate actuation for alleviation of whirl–flutter instability of the full-scale XV-15 proprotor on a semispan wing. Wing-flaperon actuation limits are set at a ±6 deg limit and swash-plate collective and tilt inputs are each limited at ±1 deg. For either actuation scheme, full-state linear quadratic regulator optimal controllers at 458 rpm (nominal cruise rpm) and 380 kt airspeed were found to be robust to variation in airspeed, and increased the critical whirl–flutter speed of the XV-15 proprotor/semispan wing by around 85–90 kt. The controllers were robust to modest variations in rpm about the nominal cruise rpm but the wing torsion mode damping levels degraded for large increases in rotor rpm. Although the XV-15 is not designed to see such large increases in rpm in the cruise mode, the results suggest that if large rpm variations in cruise were desired, rpm-scheduled controllers might be required. For either actuation scheme, controllers based on the feedback of wing states alone performed comparably to the full-state feedback controllers. Thus, output feedback based on a few, easily measurable wing states appears to be viable.

Nomenclature

F^a	=	vector of loads due to active control inputs
$[G_{\text{sp}}]$	=	control gain matrix for swash-plate actuation
$[G_\delta]$	=	control gain vector for wing-flaperon actuation
J	=	LQR optimal control cost function
$[M]$, $[C]$, $[K]$	=	proprotor-wing mass, damping, stiffness matrices
$[Q]$	=	penalty associated with system states in LQR optimal control
q	=	rotor-wing degree-of-freedom vector
R	=	penalty associated with active control inputs in LQR optimal control
u	=	active control actuation input
v	=	wing-tip chordwise bending (chord) degree of freedom
w	=	wing-tip vertical bending (beam) degree of freedom
$\bar{x}$	=	vector of rotor-wing states for the XV-15 semispan model
β_G, β, ζ	=	gimbal motion, blade flap motion, blade lag motions
β_0, β_{1c}, β_{1s}	=	rotor collective, longitudinal cyclic, and lateral cyclic flapping degrees of freedom
δ	=	wing-flaperon deflection (active control input)
$\zeta_{\min}$	=	damping ratio of the least damped mode (used in determining wing-state feedback gains through parametric optimization)
ζ_0, ζ_{1c}, ζ_{1s}	=	rotor collective, longitudinal cyclic, and lateral cyclic lag degrees of freedom
θ_a	=	active cyclic pitch input through swash plate
$\lvert\theta_{\text{cycl}}\rvert = \sqrt{\theta_{1c}^2 + \theta_{1s}^2}$	=	swash-plate cyclic motion amplitude or swash-plate tilt magnitude
θ_0, θ_{1c}, θ_{1s}	=	swash-plate collective and cyclic pitch (active control inputs)
ϕ	=	wing-tip torsion degree of freedom
ψ_s	=	rotor speed degree of freedom

Presented as Paper 2074 at the 46th AIAA/ASME/ASCE/AHS/ASC Structures, Structural Dynamics and Materials Conference, Austin, Texas, 18–21 April 2005; received 24 September 2005; revision received 21 May 2007; accepted for publication 3 June 2007.

*Graduate Research Assistant, Aerospace Engineering Department, 229 Hammond Building.
†Professor, Aerospace Engineering Department, 229 Hammond Building. Senior Member AIAA.
‡Engineer, Flying Qualities Department.

I. Introduction

TILTROTOR whirl–flutter instability has been the focus of considerable analytical and experimental research. The fundamental cause of the instability, destabilizing in-plane hub forces generated by the airloads required to precess the rotor, has been well understood for some time. The conventional approach to ensuring adequate whirl–flutter stability margins has required wing structures with very high torsional stiffness. This stiffness requirement leads to rather thick wing sections with associated high levels of aerodynamic drag, reducing the aircraft's range and efficiency. Although passive design techniques can improve tiltrotor aeroelastic stability, there may be limits to this approach, particularly in the case of soft in-plane rotor configurations, which are being considered for future tiltrotor designs. For instance, Howard [1] reported that for soft in-plane tiltrotors, combinations of rotor aeroelastic couplings or wing structural couplings that alleviate air resonance may be detrimental to whirl–flutter stability. Furthermore, the few soft in-plane configurations that have been tested in a wind tunnel (see [2,3]) have exhibited unacceptably low levels of wing vertical bending mode damping, which passive design changes alone may not be able to improve. Another option for improving tiltrotor aeroelastic stability is the use of active controls, and there have been several studies that have addressed this subject [2–13].

During a test of the Boeing model 222 soft in-plane rotor in the NASA Ames 40- by 80-ft wind tunnel, a simple feedback control system to increase damping of the poorly damped wing vertical bending mode was investigated [2]. An accelerometer mounted on the wing tip sensed vertical bending motion of the wing. Active control inputs to the system were introduced through the swash plate. After an open-loop study to determine the best gain and phase for the controller, closed-loop tests were conducted. The controller was very successful at adding damping to the wing vertical bending mode.

In [4], Johnson analytically investigated the use of an optimal controller with an estimator for reduction of tiltrotor gust response for both the Boeing and Bell full-scale rotors tested at NASA Ames in the early 1970s. The actuation strategies considered included active flaperons, swash-plate inputs, and a combination of the two. Both flaperons and swash-plate-based controllers were effective at improving proprotor gust response. Because the lowly damped wing modes were an important part of the gust response, the controller acted to greatly increase the damping of the wing modes to reduce the response. Thus, although Johnson in [4] did not explicitly consider the problem of aeroelastic instability, it did confirm that active control was a feasible technique for tiltrotor damping augmentation.

Studies by Nasu [5] and van Aken [6,7] analytically demonstrated the ability of a simple feedback control system using swash-plate actuation to influence whirl–flutter stability. No attempt was made in these studies to optimize the performance of the active control system. In [8], Vorwald and Chopra used optimal control techniques to improve whirl–flutter stability. A linear quadratic regulator (LQR) optimal controller with observer commanding inputs through the swash plate was formulated. A significant increase in predicted flutter speed was obtained, but no consideration was given as to whether the control inputs commanded by the controller were within physically realistic limits.

More recently, a great deal of experimental work [3,9–11] has been performed at NASA Langley Research Center and Bell Helicopters to evaluate the effectiveness of a modern adaptive control algorithm known as generalized predictive control (GPC) for tiltrotor stability augmentation and vibration suppression. GPC is a digital time-domain multi-input, multi-output predictive control method [12]. System identification and control input calculations are performed online. The active control inputs are through the swash plate. These experimental investigations have demonstrated the potential of a GPC-based controller to improve tiltrotor aeroelastic and aeromechanical stability. However, complex adaptive control algorithms such as GPC are not attractive for use in production aircraft due to the high cost of developing and certifying such a system.

From the above, it is evident that tiltrotor active aeroelastic stability augmentation efforts have largely focused on using swash-plate-based actuation, with little attention to actuation via a wing flaperon. An active wing flaperon, with large control authority in high-speed cruise, is an attractive candidate for increasing tiltrotor whirl–flutter stability boundaries, and has been considered for reduction of tiltrotor vibratory loads reduction [14]. Further, although the control algorithms examined varied considerably in terms of sophistication—from simple (even single state) unoptimized feedback controllers, which served to demonstrate the feasibility of active control, to complex adaptive control systems—very limited work has been done with full-state LQR optimal controllers. An LQR optimal controller provides a useful benchmark as it establishes the maximum possible stability augmentation, against which the performance of both simple as well as complex GPC-adaptive controllers can be evaluated. Consequently, the third and fourth authors of this paper, most recently conducted a preliminary study on the effectiveness of a wing-flaperon based actuation system for whirl–flutter alleviation, using an LQR optimal control algorithm [13].

Based on the full-scale XV-15 proprotor/semispan wing model the objectives of the present analytical study are threefold:

1) To compare the effectiveness of wing-flaperon based actuation versus swash-plate-based actuation for whirl–flutter stability augmentation.

2) To examine the robustness of active control, for both actuation concepts, for variations in flight speed and rotor RPM.

3) To examine the effectiveness of simple output feedback controllers, vis à vis a full-state optimal controller. How effective is control, based on feedback of a few, key easily measured wing states, relative to the performance of a full-state controller?

II. Brief Description of Analytical Model and Approach

A. Overview of Analytical Model

The analytical model used in the present investigation was developed in [15], and its essential features are described briefly. The model represents a single proprotor mounted on a semispan, cantilevered wing structure (Fig. 1a). Rigid-blade flap and lag motions (see Fig. 1) occur about spring-restrained offset hinges. The model allows for the distribution of blade flap and lag flexibility inboard and outboard of the pitch bearing. As a result, variations in rotor frequencies and pitch-flap and pitch-lag couplings which occur with changes in collective pitch can be captured from first principles. In contrast, other rigid-blade tiltrotor stability analyses typically rely upon tabulated input data to represent these variations in rotor frequency and couplings. In addition to an in-depth description of the features of the analytical model, and a discussion of the impact of these features on whirl–flutter stability prediction, Hathaway and Gandhi [15] provide extensive validation results with existing elastic blade tiltrotor stability analyses as well as experimental test data, for several different tiltrotor configurations. The validated analysis has already been used in initial studies on the influence of a wing flaperon in alleviating whirl–flutter instability [13], as well as design optimization studies to passively improve tiltrotor aeroelastic stability [16].

After transforming the rotor blade equations into the nonrotating system using multiblade coordinate transformation the rotor-wing equations of motion are written as

$$[M]\ddot{q} + [C]\dot{q} + [K]q = F^a \tag{1}$$

where $[M]$, $[C]$, and $[K]$ are the rotor-wing mass, damping, and stiffness matrices (including aerodynamic contributions), q is the vector of rotor and wing degrees of freedom, and F^a represents the loads generated due to active control. Further details can be obtained in [17].

B. Active Control Using Wing Flaperon

One of the mechanisms for implementation of active control inputs is through deflection δ of the wing flaperon. In the present study, the flaperon is sized to approximately match the XV-15's flaperon, with a chord equal to 25% of the total wing chord, and a span covering the outer 50% of the wing (schematically depicted in Fig. 2). Using a quasi-steady aerodynamics assumption, the active control loads generated due to deflection of the wing flaperon can simply be expressed in the form

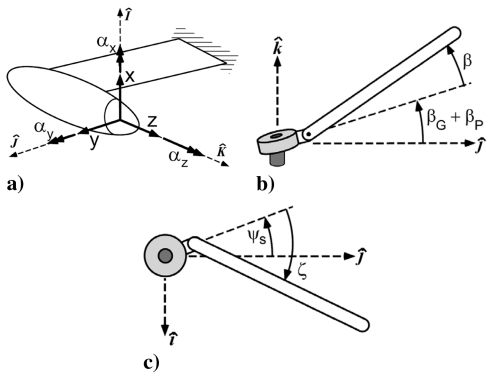

Fig. 1 a) Proprotor (hub) on semispan wing. Degrees of freedom at hub attachment point. b) Gimbal and blade flapping degrees of freedom. c) Rotor azimuthal and blade lead–lag degrees of freedom.

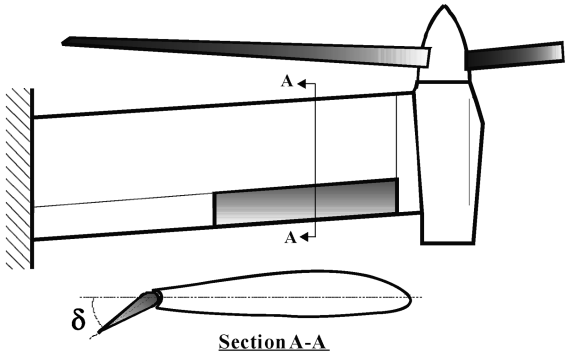

Fig. 2 Schematic of wing-flaperon actuation.

$$F^a = [D_\delta]\delta \tag{2}$$

Detailed expressions for active control loads using full unsteady aerodynamics are available in [13,17], but it was shown in these references that a quasi-steady aerodynamic model is generally quite adequate. Wing-flaperon deflection is related to the rotor-wing states $\bar{x}$, using the feedback control law

$$\delta = -[G_\delta]\{\bar{x}\} \tag{3}$$

where the vector $[G_\delta]$ of control gains is determined by the controller design process.

C. Active Control Using the Swash Plate

Another mechanism considered for implementation of active control inputs is through the swash plate (see schematic representation in Fig. 3). The active pitch input through the swash plate is expressed as

$$\theta_a = \theta_0 + \theta_{1c}\cos\psi + \theta_{1s}\sin\psi \tag{4}$$

and the active control loads (aerodynamic loads) generated due to swash-plate actuation can be expressed in the form

$$F^a = [D_{\text{sp}}]\begin{Bmatrix}\theta_0\\ \theta_{1c}\\ \theta_{1s}\end{Bmatrix} \tag{5}$$

Swash-plate actuation inputs are related to the rotor-wing states $\bar{x}$, using the feedback control law

$$\begin{Bmatrix}\theta_0\\ \theta_{1c}\\ \theta_{1s}\end{Bmatrix} = -[G_{\text{sp}}]\bar{x} \tag{6}$$

where $[G_{\text{sp}}]$ is the matrix of control gains, to be determined by the controller design process.

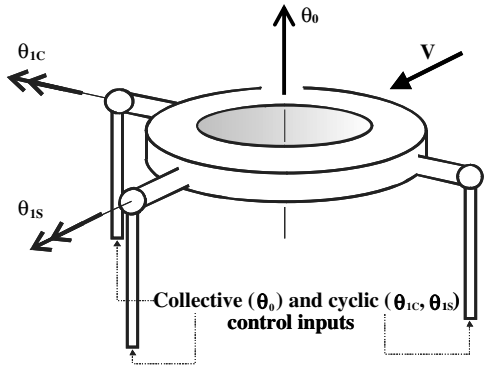

Fig. 3 Schematic of swash-plate actuation.

D. Limits on Control Gains

An important issue in evaluating the effectiveness of an active control scheme is actuation authority. A given set of controller gains may be able to completely eliminate whirl flutter, but if that controller commands flaperon deflections or swash-plate inputs that exceed the practical limits, then the performance improvements predicted (increase in whirl–flutter critical speed or increase in damping of specific modes) have no practical significance. Limits on the controller gains can be introduced by considering both the magnitude of perturbations the system is likely to encounter as well as the limits on the flaperon and swash-plate deflections, themselves. Based on [14], it is assumed that nominally the available flaperon deflection for stability augmentation is ±6 deg, and the available swash-plate collective and cyclic motion amplitudes are each ±1 deg. The swash-plate cyclic motion amplitude, or the swash-plate tilt, is calculated using

$$|\theta_{\text{cycl}}| = \sqrt{\theta_{1c}^2 + \theta_{1s}^2} \tag{7}$$

and the constraints on available actuation are then represented mathematically as

$$|\delta| \le 6 \text{ deg}, \qquad |\theta_0| \le 1 \text{ deg} \quad \text{and} \quad |\theta_{\text{cycl}}| \le 1 \text{ deg} \tag{8}$$

Consider a linear feedback system with the control law expressed as

$$u = -[G]\bar{x} \tag{9}$$

where u is the actuation input (δ for flaperon actuation, or the vector $\lfloor\theta_0 \;\; \theta_{1c} \;\; \theta_{1s}\rfloor^T$ for swash-plate actuation), and $[G]$ is the controller gain matrix ($[G_\delta]$ for flaperon actuation, or $[G_{\text{sp}}]$ for swash-plate actuation). It is evident from Eq. (9) that for a specified maximum limit on u, the controller gain matrix $[G]$ is limited by $\bar{x}$. The larger the disturbance levels (larger $\bar{x}$), the tighter the limits on the controller gain matrix, and vice versa. Thus, for a controller designed for practical implementation, a worst-case disturbance condition must be identified, and controller gains limited to prevent the control input u from exceeding the prescribed limits for this disturbance.

The state vector $\bar{x}$ corresponding to the XV-15 semispan model is given by

$$\bar{x} = [\dot{w} \;\; \dot{v} \;\; \dot{\phi} \;\; \dot{\beta}_0 \;\; \dot{\beta}_{1c} \;\; \dot{\beta}_{1s} \;\; \dot{\zeta}_0 \;\; \dot{\zeta}_{1c} \;\; \dot{\zeta}_{1s} \;\; \dot{\psi}_s \;\; \dot{\beta}_{Gc} \;\; \dot{\beta}_{Gs} \;\; w \;\; v \;\; \phi \;\; \beta_0 \;\; \beta_{1c} \;\; \beta_{1s} \;\; \zeta_0 \;\; \zeta_{1c} \;\; \zeta_{1s} \;\; \beta_{Gc} \;\; \beta_{Gs}]^T \tag{10}$$

where β_0, β_{1c}, and β_{1s} are the rotor flap degrees of freedom in the nonrotating system, and ζ_0, ζ_{1c}, and ζ_{1s} are the rotor lag degrees of freedom in the nonrotating system. The wing-tip degrees of freedom w (vertical bending displacement), v (lag bending displacement), and ϕ (wing-tip torsion) can be related to the rotor hub degrees of freedom in Fig. 1.

For the present study it is assumed that disturbances would cause the following maximum wing-tip deformations for the semispan tiltrotor model: wing-tip displacements of 2.5% of the rotor radius vertically, 1% of the rotor radius in the chordwise direction, and torsional rotation of 1 deg. The control gains selected for the results in this study ensure that for the perturbations considered above, the resulting wing-flaperon/swash-plate inputs do not exceed the maximum limits placed on them.

E. Evaluation of LQR Optimal Controller Gains for Full-State Feedback

An LQR optimal controller is implemented which determines a set of controller gains that minimizes the following cost function:

$$J = \int_0^\infty (\bar{x}^T[Q]\bar{x} + u^T R u)\,\mathrm{d}t \tag{11}$$

The value of the weight on the control effort R is iteratively adjusted to allow the largest possible increase in flutter speed, without exceeding the actuation limits described previously. The optimal

controller gains are easily determined by solving the system algebraic Riccati equation. The optimal controller gains depend on the plant or model parameters, which vary, for example, with flight speed or rotor rpm. As the aircraft cruise speed increases, the best performance is obtained with a controller that is scheduled with respect to airspeed. However, this increases the complexity of the controller, and it would be highly advantageous if a constant-gain controller were effective over a broad range of conditions (implying that the controller is robust).

F. Evaluation of Controller Gains for Output (Wing-State) Feedback Using Parametric Optimization

Using full-state LQR optimal control allows determination of the maximum possible improvement in the aeroelastic stability. However, full-state feedback is difficult to implement because all system states are not generally easily measurable. Furthermore, examining the LQR full-state optimal control gain matrix, it was observed that the control gains corresponding to feedback of wing states were dominant. This suggests using output feedback based on a few, easily measured wing states. One approach would be to measure the wing states and use an estimator for the rest of the system states, but this significantly increases the problem complexity (as compared to the straightforward solution of an algebraic Riccati equation for the case of full-state feedback). Another approach, used in this paper, is to consider the controller gains corresponding to the wing states as design variables and conduct a parametric optimization to determine the values of those gains, corresponding to a specified objective function. The optimization is set up to increase the level of damping in the *least* damped mode at an airspeed where the baseline (uncontrolled) system is unstable. Specifically, the objective function used was

$$\text{maximize } F(G_j) = \zeta_{\min}|_{380 \text{ kt},458 \text{ rpm}} \tag{12}$$

where G_j are the control gains (design variables) and $\zeta_{\min}$ is the damping ratio of the least damped mode at a target airspeed of 380 kt. The optimization is carried out at a rotor speed of 458 rpm, the nominal cruise mode rpm of the XV-15. Each iteration in the optimization procedure involves conducting an eigenanalysis, identifying $\zeta_{\min}$, calculating sensitivity gradients, $\partial\zeta_{\min}/\partial G_j$, by numerical perturbation of the design variables (controller gains), then updating the design variables (controller gains), and repeating this process until optimality is achieved.

III. Results

As mentioned previously, numerical simulations in the present study are based on the stiff in-plane XV-15 semispan model. Key model parameters of this configuration are given in Table 1. Figure 4 shows the plots of the baseline modal damping (no active control), as a function of airspeed, and at a rotational speed of 458 rpm (the cruise rpm of the XV-15 proprotor). Note that the collective pitch changes with airspeed as the model is trimmed to zero torque (windmilling condition) at each airspeed. Whirl–flutter instability is encountered at an airspeed of 330 kt where the wing vertical bending mode (the "beam mode") damping is zero. Figure 5 shows the modal damping variation, as a function of rpm, at an airspeed of 380 kt (an arbitrarily selected target cruise speed up to which we would like the system to be free of whirl–flutter instability with the use of active control). Because this speed is greater than the critical flutter speed for the baseline (no-control) system, certain modes are seen to have negative damping.

A. Full-State LQR Control—Airspeed-Scheduled and Constant-Gain Controllers

1. Wing-Flaperon Actuation

The influence of wing-flaperon actuation based on full-state LQR optimal control is shown in Fig. 6. The rotational speed is 458 rpm and the optimal control gains are *scheduled with respect to airspeed*. Full-state LQR optimal control ensures stability, and so the damping

Table 1 XV-15 full-scale model properties

Number of blades, N	3
Rotor radius, R	12.5 ft
Lock no., γ	4.06
Solidity, σ	0.089
Lift curve slope, $C_{l\alpha}$	5.7
Rotor rpm, Ω	458 rpm (cruise) 565 rpm (hover)
Pitch-gimbal coupling, K_{PG}	−0.268
Inertia properties	
I_b	105 slug-ft^2
I_β	81.8 slug-ft^2
$I_{\beta\alpha}$	105 slug-ft^2
I_ζ	70.4 slug-ft^2
$I_{\zeta\alpha}$	82.6 slug-ft^2
S_β	10.2 slug-ft
S_ζ	8.69 slug-ft
Blade stiffness	
$\omega_{\beta 0}$	59.8 rad/s
$\omega_{\zeta 0}$	103 rad/s
R_β	1
R_ζ	1

in the various modes never becomes negative. The critical speed, then, is the speed at which the flaperon deflections required exceed the prescribed limits (assumed to be ±6 deg). The value of the weighting parameter R in Eq. (11) is adjusted iteratively, to simultaneously increase the critical flutter speed and maintain greater than about 1% damping in the three wing modes. The critical speed is increased to 415 kt, at which point the flaperon deflections exceed the

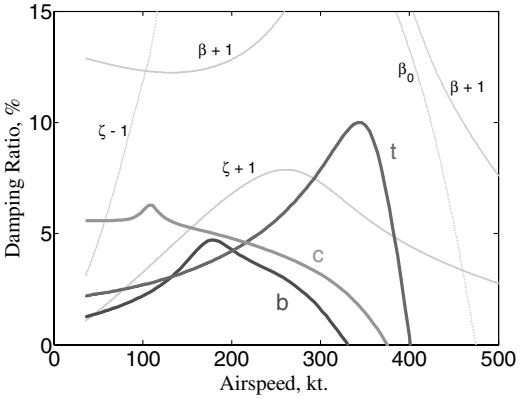

Fig. 4 458 rpm, modal damping vs airspeed, baseline, no-control case (b = wing beam mode, c = wing chord mode, and t = wing torsion mode).

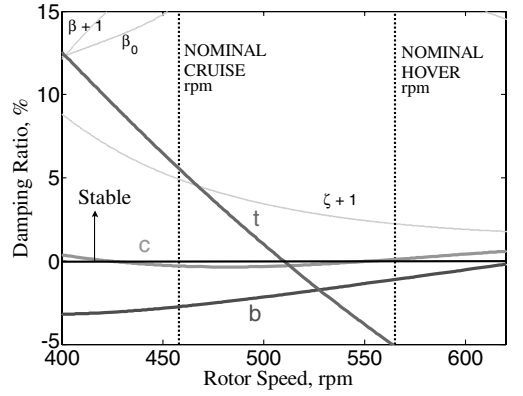

Fig. 5 380 kts, modal damping vs rpm, baseline, no-control case (b = wing beam mode, c = wing chord mode, and t = wing torsion mode).

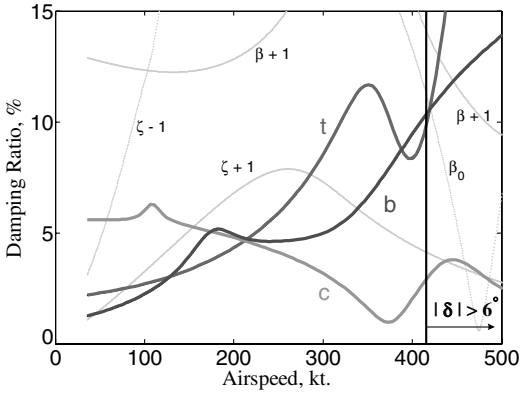

Fig. 6 458 rpm, modal damping vs airspeed with wing-flaperon actuation, airspeed-scheduled full-state LQR optimal control.

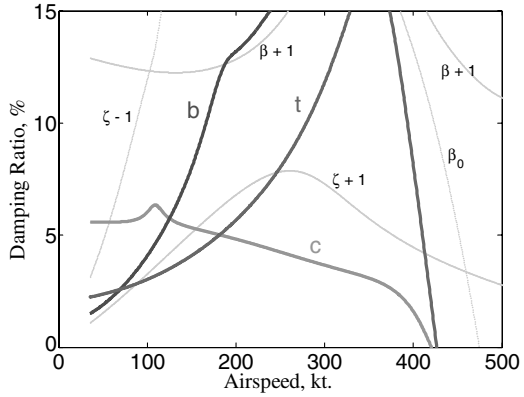

Fig. 7 458 rpm, modal damping vs airspeed with wing-flaperon actuation, constant-gain control (full-state LQR optimal controller at 380 kt, 458 rpm applied at all airspeeds).

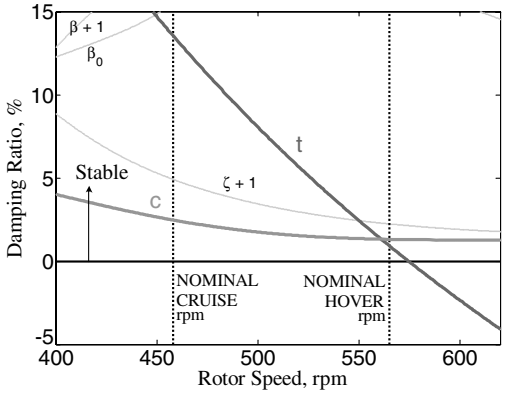

Fig. 8 380 kt, modal damping vs rpm with wing-flaperon actuation, constant-gain control (full-state LQR optimal controller at 380 kt, 458 rpm applied at all rotor speeds).

±6 deg limit. This represents an 85 kt increase over the 330 kt critical flutter speed for the baseline (Fig. 4). A reduction in wing chord mode damping around 370 kt is observed in Fig. 6. This corresponds to the airspeed at which the wing chord mode goes unstable for the baseline system. In the presence of active control, the reduction in damping is also related to the limits placed on the wing-flaperon deflection, and relaxing the limits results in an increase in wing chord mode damping.

Next, from Fig. 6, the LQR optimal gains at 380 kt airspeed (Table 2) are used over the entire airspeed range to examine the effect of using a constant-gain controller (as opposed to the airspeed-scheduled controller in Fig. 6). The corresponding modal damping values, as a function of airspeed, are shown in Fig. 7. It is seen that flutter instability is encountered at around 420 kt, at which point the wing chordwise bending mode becomes unstable. This represents an increase of 90 kt over the baseline value of 330 kt (compare to Fig. 4), with the flaperon deflections remaining less than ±6 deg at subcritical speeds.

Figure 8 shows the effect of the 380-kt, 458-rpm optimal gain vector (used in Fig. 7) over a 400–620 rpm range (and at 380 kt airspeed). The modal damping levels show a vast overall improvement relative to the baseline (uncontrolled) case (compare to Fig. 4). The flaperon deflections in Fig. 8 remain below the ±6 deg limit over the entire rpm range considered. In cruise condition, the rotor is expected to operate at or around the nominal cruise rpm of 458 rpm. It is observed that around the nominal cruise rpm all the modes remain stable, and damping in the wing chord mode is around 2.5%. At much higher rotational speeds the damping in the wing chord mode decreases to around 1.5%. With an increase in rotational speed, the wing torsion mode damping reduces more rapidly and the mode becomes unstable at 575 rpm. Although this is close to the nominal hover rotor speed of 565 rpm, the rotor is not designed to operate at these speeds in cruise. However, if rotor speed variation was desired in the airplane mode, an active controller designed at the nominal cruise rpm would be "off design" at higher rotational speeds and the performance degradation, depending on the range of rpm variation sought, might be unacceptable. In that case, an rpm-scheduled controller would be required, at the very least.

Table 2 Gain matrix from LQR at 380 kt, 458 rpm

State variables	Control input θ_0	θ_{1c}	θ_{1s}	δ
$\dot{\boldsymbol{w}}$	**0.0648**	**0.4440**	**0.1108**	**3.8583**
$\dot{\boldsymbol{v}}$	**0.3091**	**0.0552**	**−0.0765**	**2.7040**
$\dot{\boldsymbol{\phi}}$	**−0.0052**	**0.0341**	**0.0482**	**−0.4573**
$\dot{\beta}_0$	−0.0010	0.0028	−0.0037	0.1281
$\dot{\beta}_{1c}$	0.0013	0.0527	0.0129	−0.0069
$\dot{\beta}_{1s}$	−0.0045	−0.0125	0.0503	−0.1178
$\dot{\zeta}_0$	0.0578	−0.0003	0.0017	−0.0836
$\dot{\zeta}_{1c}$	0.0022	0.0068	−0.0030	−0.0047
$\dot{\zeta}_{1s}$	0.0008	0.0046	0.0096	−0.1172
$\dot{\psi}_s$	−0.0073	0.0004	−0.0021	0.1079
$\dot{\beta}_{Gc}$	0.0015	0.0168	0.0146	−0.0110
$\dot{\beta}_{Gs}$	−0.0051	−0.0142	0.0142	−0.1339
$\boldsymbol{w}$	**0.0442**	**0.0496**	**0.2028**	**0.0056**
$\boldsymbol{v}$	**0.3001**	**0.1131**	**0.0071**	**−1.0943**
$\boldsymbol{\phi}$	**−0.0007**	**−0.0448**	**0.0530**	**−0.4547**
β_0	−0.0131	0.0031	−0.0007	−0.0473
β_{1c}	0.0052	0.0877	0.0074	0.1691
β_{1s}	0.0016	0.0007	0.0899	−0.1754
ζ_0	0.0911	0.0005	−0.0005	−0.0070
ζ_{1c}	0.0047	0.0300	−0.0084	0.1186
ζ_{1s}	−0.0020	0.0182	0.0128	−0.2186
β_{Gc}	0.0050	0.0258	−0.0146	0.2067
β_{Gs}	0.0019	0.0231	0.0281	−0.1655

2. *Swash-Plate Actuation*

For the case of swash-plate actuation, performance of the optimal LQR controller scheduled with airspeed is shown in Fig. 9 (corresponding to the nominal cruise rpm of 458 rpm). The stability boundary is increased by about 70 kt, from the baseline value of 330 kt (Fig. 4) to about 400 kt, at which point the ±1 deg limit on the swash-plate tilt is exceeded. A reduction in wing beam mode damping around 330 kt is observed in Fig. 9, corresponding to the airspeed at which the wing beam mode goes unstable for the baseline system. In the presence of active control, the reduction in damping is related to the limits placed on the swash-plate collective and tilt, and relaxing the limits results in an increase in wing beam mode damping.

Next, from Fig. 9, the optimal gains at 380 kt airspeed (Table 2) are used over the entire airspeed range to examine the effect of using a

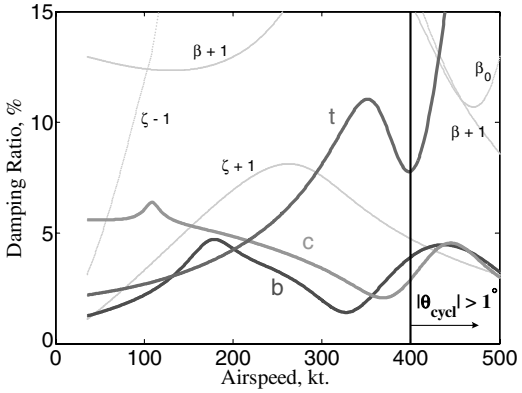

Fig. 9 458 rpm, modal damping vs airspeed with swash-plate actuation, airspeed-scheduled full-state LQR optimal control.

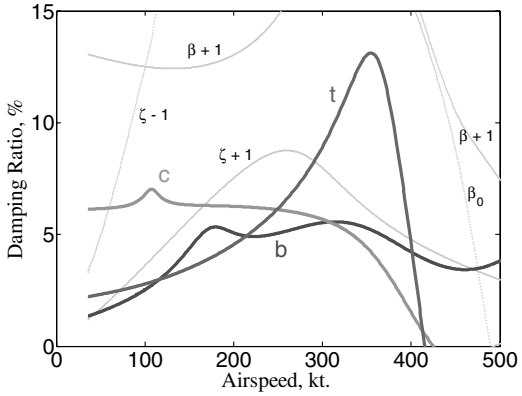

Fig. 10 458 rpm, modal damping vs airspeed with swash-plate actuation, constant-gain control (full-state LQR optimal controller at 380 kt, 458 rpm applied at all airspeeds).

constant-gain controller (as opposed to the airspeed-scheduled controller in Fig. 9). The corresponding modal damping values, as a function of airspeed, are shown in Fig. 10. It is seen that flutter is encountered at around 415 kt, at which point the wing torsion mode becomes unstable. This represents an 85 kt increase over the baseline value of 330 kt (compare to Fig. 4). The swash-plate collective and tilt angles in Fig. 10 remain below the ± 1 deg limit at all airspeeds in the subcritical range.

Figure 11 shows the effect of the 380-kt, 458 rpm optimal gain matrices (used in Fig. 10) over a 400–620 rpm range (and at 380 kt airspeed). The modal damping levels show a vast overall improvement relative to the baseline (uncontrolled) case (compare to Fig. 4). The swash-plate collective and tilt in Fig. 11 remain below the ± 1 deg limit over the entire rpm range considered. At or around the nominal cruise rpm of 458 rpm, the wing chord mode damping is seen to be around 3%, and the damping in the wing beam and torsion modes is even larger. With an increase in rotational speed, the wing torsion mode damping reduces and the mode becomes unstable at around 555 rpm. It should be noted, though, that the rotor is not designed to operate at these speeds in cruise. The results do suggest, however, that if large rotor speed variation is to be used in airplane mode, an rpm-scheduled controller might be necessary to negate the performance degradation of an active controller designed at the nominal cruise rpm which would be badly off design at the higher rotational speeds.

The increase in flutter speed obtained with active control is really due to an increase in modal damping. The destabilizing aerodynamic forces are partially negated due to the feedback control implemented through the wing flaperon or the swash plate.

B. Optimization with Output (Wing-State) Feedback

In this section controllers based on feedback of a few key states are examined. This is because output feedback of a few easily measured states is more practical than full-state feedback. Further, in Table 2 it is seen that even with full-state feedback, the control gains corresponding to the six wing states (wing-tip positions, w, v, and ϕ, and velocities, $\dot{w}$, $\dot{v}$, and $\dot{\phi}$) were the dominant gains. This suggests that the performance of a controller based on the feedback of wing states alone may be comparable to that of a full-state feedback controller.

1. Wing-Flaperon Actuation

For wing-flaperon actuation, Fig. 12 shows modal damping versus airspeed of a wing-state feedback controller designed using the parametric optimization procedure described previously and the objective function in Eq. (12) (maximizing the damping of the least damped mode at 380 kt airspeed and 458 rpm rotor speed). The critical whirl–flutter speed is 425 kt, which represents a 95 kt increase over the baseline (Fig. 4), and is comparable to that obtained with a full-state feedback constant-gain controller (Fig. 7). The flaperon deflections corresponding to the modal damping results in Fig. 12 remain below the ± 6 deg limit. The optimal control gains are given in Table 3, and the performance of this controller is slightly better than an ad hoc controller that uses just the highlighted gains from Table 2 (modal damping results of the ad hoc controller are not shown, but the resulting critical flutter speed is 390 kt).

Figure 13 shows the effect of the 380-kt, 458-rpm optimized gain vector over a 400–620 rpm range (and at 380 kt airspeed). The flaperon deflections in Fig. 13 remain below the ± 6 deg limit over the entire rpm range considered. Around the nominal cruise rpm of 458 rpm all the wing modes are observed to have adequate damping levels, with the lowest damped wing chord mode at over 3.5%. At much higher rotational speeds, there is a significant reduction in wing torsion mode damping and this mode goes unstable around 580 rpm.

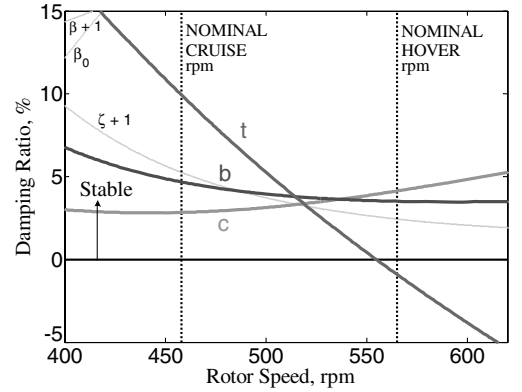

Fig. 11 380 kt, modal damping vs rpm with swash-plate actuation, constant-gain control (full-state LQR optimal controller at 380 kt, 458 rpm applied at all rotor speeds).

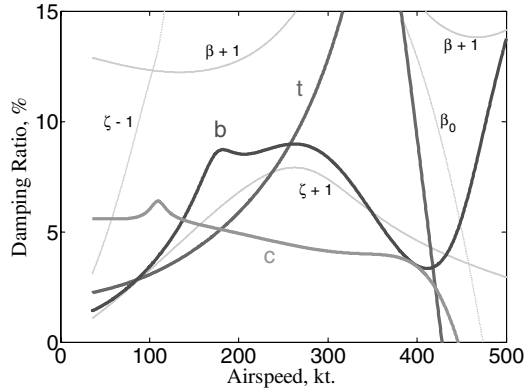

Fig. 12 458 rpm, modal damping vs airspeed with wing-flaperon actuation based on wing-state feedback (constant controller gains determined by parametric optimization at 380 kt, 458 rpm).

Table 3 Gain matrix from optimization at 380 kt, 458 rpm (wing-states feedback)

State variables	Control input			
	θ_0	θ_{1c}	θ_{1s}	δ
$\dot{w}$	−0.9478	0.2302	−0.1831	5.5741
$\dot{v}$	0.1026	−0.5132	−0.3447	6.5506
$\dot{\phi}$	0.4481	0.2959	0.1155	−0.1554
w	−0.1800	−0.5920	0.3897	2.2166
v	0.4354	0.2726	0.2517	−6.4328
ϕ	0.0374	−0.1472	0.2436	−3.6738

However, in cruise condition, the rotational speed is expected to remain in the vicinity of the nominal cruise speed (458 rpm).

Comparing the results in Figs. 12 and 13 to those in Figs. 7 and 8, respectively, it is evident that using wing-flaperon actuation, the performance of a controller based on wing-state feedback alone is comparable to that of a full-state feedback controller.

2. Swash-Plate Actuation

For swash-plate actuation, Fig. 14 shows the modal damping versus airspeed of a wing-state feedback controller designed using the parametric optimization procedure described previously and the objective function in Eq. (12) (maximizing the damping of the least damped mode at 380 kt airspeed and 458 rpm rotor speed). The critical whirl–flutter speed is 410 kt, which represents an 80 kt increase over the baseline (Fig. 4), and is comparable to that obtained with a full-state feedback constant-gain controller (Fig. 10). The swash-plate collective and cyclic inputs corresponding to the modal damping results in Fig. 14 remain below the ±1 deg limits. The optimal control gains are given in Table 3, and the performance of this controller is slightly better than an ad hoc controller that uses just the highlighted gains from Table 2 (modal damping results of the ad hoc controller are not shown, but the resulting critical flutter speed is 395 kt).

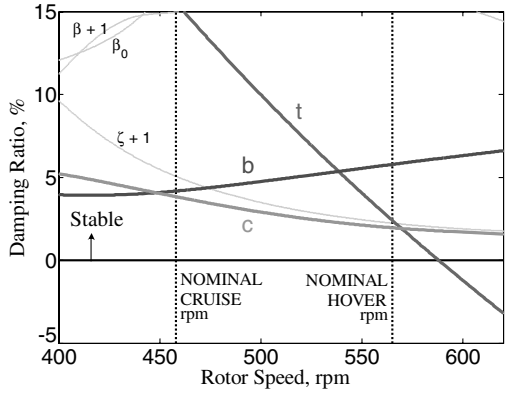

Fig. 13 380 kt, modal damping vs rpm with wing-flaperon actuation based on wing-state feedback (constant controller gains determined by parametric optimization at 380 kt, 458 rpm).

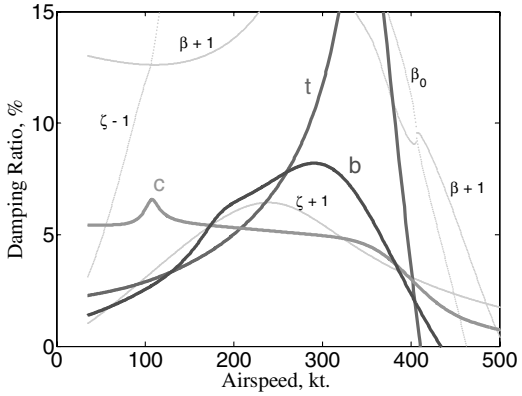

Fig. 14 458 rpm, modal damping vs airspeed with swash-plate actuation based on wing-state feedback (constant controller gains determined by parametric optimization at 380 kt, 458 rpm).

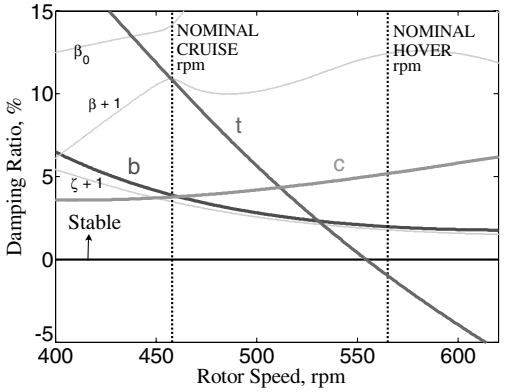

Fig. 15 380 kt, modal damping vs rpm, with swash-plate actuation based on wing-state feedback (constant controller gains determined by parametric optimization at 380 kt, 458 rpm).

Figure 15 shows the effect of the 380-kt, 458-rpm optimized gain vector over a 400–620 rpm range (and at 380 kt airspeed). The swash-plate collective and cyclic inputs in Fig. 15 remain below the ±1 deg limits over the entire rpm range considered. Around the nominal cruise rpm of 458 rpm all the wing modes are observed to have adequate damping levels, with the lowest damped wing modes at over 3.5%. At much higher rotational speeds, there is a significant reduction in wing torsion mode damping and this mode goes unstable around 550 rpm. However, in cruise condition, the rotational speed is expected to remain in the vicinity of the nominal cruise speed (458 rpm).

Comparing the results in Figs. 14 and 15 to those in Figs. 10 and 11, respectively, it is evident that using swash-plate actuation, the performance of a controller based on wing-state feedback alone is comparable to that of a full-state feedback controller.

IV. Conclusions

For the full-scale XV-15 proprotor on a semispan wing, the present paper examined the influence of active control in alleviating whirl–flutter instability. Active control inputs were introduced through the wing flaperon or the swash plate, and the inputs were based on full-state feedback or output feedback of wing states, alone. A ±6 deg limit was imposed on flaperon actuation inputs and ±1 deg limits were imposed on swash-plate collective and tilt inputs.

For wing-flaperon actuation, full-state LQR optimal control gains at 458 rpm (nominal cruise speed) and 380 kt were found to be robust to variations in airspeed. These controller gains increased the critical whirl–flutter speed by 90 kt, relative to the uncontrolled system, with flaperon deflections remaining under the prescribed limit before the onset of flutter. The controller performed well with modest variation in rotor rpm about the nominal cruise rpm, but for large increases in rotor rpm the wing torsion mode damping, in particular, showed degradation. For swash-plate actuation, also, full-state LQR optimal control gains at 458 rpm (nominal cruise speed) and 380 kt were found to be robust to variations in airspeed. These controller gains increased the critical whirl–flutter speed by 85 kt, relative to the uncontrolled system, with swash-plate collective and tilt remaining under the prescribed limit before the onset of flutter. As with wing-flaperon actuation, the controller performed well with modest variation in rotor rpm about the nominal cruise rpm, but for large increases in rotor rpm the wing torsion mode damping showed degradation. This suggests that for either flaperon or swash-plate actuation, if a fairly large rpm variation is to be used in the cruise mode, an rpm-scheduled controller might be required.

From the full-scale LQR optimal gain matrices it was observed that gains corresponding to feedback of wing states were dominant. This led to examining the influence of output feedback based on wing states alone. The controller gains were determined using parametric optimization to maximize the damping of the least damped mode at a specified cruise speed and rotor rpm. Results indicate that for both the wing flaperon as well as the swash-plate actuation, a constant-gain controller based on feedback of wing states alone is comparable in performance to a full-state feedback controller. The wing-state feedback controllers show similar increases in whirl–flutter speed, subcritical damping levels, and robustness to variation in airspeed and rotor rpm.

Acknowledgments

This research is funded by the National Rotorcraft Technology Center (NRTC) under the Penn State Rotorcraft Center of Excellence Program, with Yung Yu serving as the technical monitor.

References

[1] Howard, A. K. T., "The Aeromechanical Stability of Soft-Inplane Tiltrotors," Ph.D. Thesis, Pennsylvania State University, University Park, PA, 2001.

[2] Magee, J. P., and Alexander, H. R., "Wind Tunnel Tests of a Full Scale Hingeless Prop/Rotor Designed for the Boeing Model 222 Tilt Rotor Aircraft," NASA CR 114664, Boeing Vertol Co., Oct. 1973.

[3] Nixon, M. W., Langston, C. W., Singleton, J. D., Piatak, D. J., Kvaternik, R. G., Corso, L. M., and Brown, R. K., "Aeroelastic Stability of a Four-Bladed Semi-Articulated Soft-Inplane Tiltrotor Model," *Proceedings of the 59th Annual AHS Forum*, The American Helicopter Society, Alexandria, VA, 6–8 May 2003.

[4] Johnson, W., "Optimal Control Alleviation of Tilting Proprotor Gust Response," *Journal of Aircraft*, Vol. 14, No. 3, March 1977, pp. 301–308.

[5] Nasu, K.-i., "Tilt-Rotor Flutter Control in Cruise Flight," NASA TM 88315, Dec. 1986.

[6] van Aken, J. M., "Alleviation of Whirl-Flutter on Tilt-Rotor Aircraft Using Active Controls," *Proceedings of the 47th Annual AHS Forum*, The American Helicopter Society, Alexandria, VA, 6–8 May 1991.

[7] van Aken, J. M., "Alleviation of Whirl-Flutter on a Joined-Wing Tilt-Rotor Aircraft Configuration Using Active Controls," *International Specialists' Meeting on Rotorcraft Basic Research of the American Helicopter Society*, The American Helicopter Society, Alexandria, VA, 25–27 March 1991.

[8] Vorwald, J. G., and Chopra, I., "Stabilizing Pylon Whirl Flutter on a Tilt-Rotor Aircraft," *Proceedings of the 32nd AIAA/ASME/ASCE/AHS/ASC Structures, Structural Dynamics, and Materials Conference*, AIAA, Washington, D.C., 8–10 April 1991.

[9] Kvaternik, R. G., Piatak, D. J., Nixon, M. W., Langston, C. W., Singleton, J. D., Bennett, R. L., and Brown, R. K., "An Experimental Evaluation of Generalized Predictive Control for Tiltrotor Aeroelastic Stability Augmentation in Airplane Mode of Flight," *Proceedings of the 57th Annual AHS Forum*, The American Helicopter Society, Alexandria, VA, 9–11 May 2001.

[10] Nixon, M. W., Langston, C. W., Singleton, J. D., Piatak, D. J., Kvaternik, R. G., Corso, L. M., and Brown, R., "Aeroelastic Stability Of A Soft-Inplane Gimballed Tiltrotor Model In Hover," *Proceedings of the 42nd AIAA/ASME/ASCE/AHS/ASC Structures, Structural Dynamics, and Materials Conference*, AIAA, Reston, VA, 16–19 April 2001.

[11] Nixon, M. W., Langston, C. W., Singleton, J. D., Piatak, D. J., Kvaternik, R. G., Corso, L. M., and Brown, R. K., "Technical Note: Hover Test of a Soft-Inplane Gimballed Tiltrotor Model," *Journal of the American Helicopter Society*, Vol. 48, No. 1, Jan. 2003, pp. 63–66.

[12] Kvaternik, R. G., "Exploratory Studies in Generalized Predictive Control for Active Aeroelastic Control of Tiltrotor Aircraft," NASA TM-2000-210552, 2000.

[13] Hathaway, E., and Gandhi, F., "Tiltrotor Whirl Flutter Alleviation Using Actively Controlled Wing Flaperons," *AIAA Journal*, Vol. 44, No. 11, Nov. 2006, pp. 2524–2534.

[14] Nixon, M. W., Kvaternik, R. G., and Settle, T. B., "Tiltrotor Vibration Reduction Through Higher Harmonic Control," *Proceedings of the 53rd Annual AHS Forum*, The American Helicopter Society, Alexandria, VA, 29 April–1 May 1997.

[15] Hathaway, E. L., and Gandhi, F., "Modeling Refinements in Simple Tiltrotor Whirl Flutter Analyses," *Journal of the American Helicopter Society*, Vol. 48, No. 3, July 2003, pp. 186–198.

[16] Hathaway, E., and Gandhi, F., "Design Optimization for Improved Tiltrotor Whirl Flutter Stability," *Journal of the American Helicopter Society*, Vol. 52, No. 2, April 2007, pp. 79–89.

[17] Hathaway, E., "Active and Passive Techniques for Tiltrotor Aeroelastic Stability Augmentation," Doctoral Thesis in Aerospace Engineering, Pennsylvania State University, University Park, PA, Aug. 2005.